



Article

Phase Synchronization and Dynamic Behavior of a Novel Small Heterogeneous Coupled Network

Mengjiao Wang ¹, Jiwei Peng ¹, Shaobo He ^{1,*}, Xinan Zhang ² and Herbert Ho-Ching Iu ²

¹ School of Automation and Electronic Information, Xiangtan University, Xiangtan 411105, China; wangmj@xtu.edu.cn (M.W.); 202121623021@smail.xtu.edu.cn (J.P.)

² School of Electrical, Electronic and Computer Engineering, University of Western Australia, Crawley, WA 6009, Australia; xinan.zhang@uwa.edu.au (X.Z.); herbert.iu@uwa.edu.au (H.H.-C.I.)

* Correspondence: hshaobo_123@163.com

Abstract: Studying the firing dynamics and phase synchronization behavior of heterogeneous coupled networks helps us understand the mechanism of human brain activity. In this study, we propose a novel small heterogeneous coupled network in which the 2D Hopfield neural network (HNN) and the 2D Hindmarsh–Rose (HR) neuron are coupled through a locally active memristor. The simulation results show that the network exhibits complex dynamic behavior and is different from the usual phase synchronization. More specifically, the membrane potential of the 2D HR neuron exhibits five stable firing modes as the coupling parameter k_1 changes. In addition, it is found that in the local region of k_1 , the number of spikes in bursting firing increases with the increase in k_1 . More interestingly, the network gradually changes from synchronous to asynchronous during the increase in the coupling parameter k_1 but suddenly becomes synchronous around the coupling parameter $k_1 = 1.96$. As far as we know, this abnormal synchronization behavior is different from the existing findings. This research is inspired by the fact that the episodic synchronous abnormal firing of excitatory neurons in the hippocampus of the brain can lead to diseases such as epilepsy. This helps us further understand the mechanism of brain activity and build bionic systems. Finally, we design the simulation circuit of the network and implement it on an STM32 microcontroller.

Keywords: Hindmarsh–Rose neuron; Hopfield neural network; heterogeneous coupled; firing patterns; phase synchronization



Citation: Wang, M.; Peng, J.; He, S.; Zhang, X.; Iu, H.H.-C. Phase Synchronization and Dynamic Behavior of a Novel Small

Heterogeneous Coupled Network. *Fractal Fract.* **2023**, *7*, 818. <https://doi.org/10.3390/fractalfract7110818>

Academic Editor: António Lopes

Received: 22 August 2023

Revised: 4 November 2023

Accepted: 8 November 2023

Published: 13 November 2023



Copyright: © 2023 by the authors. Licensee MDPI, Basel, Switzerland. This article is an open access article distributed under the terms and conditions of the Creative Commons Attribution (CC BY) license (<https://creativecommons.org/licenses/by/4.0/>).

1. Introduction

A memristor [1–5], as the fourth basic electronic component, describes the relationship between charge and magnetic flux. Due to its nanoscale, memorability, nonlinearity, and excellent bionic properties, a large number of researchers have introduced it into neural networks as a synapse [6–9] or an autapse [10], generating rich dynamic behaviors, such as coexistence [11,12] and multistability [13,14]. Memristors and chaotic systems have potential application value in the industry. He et al. applied the memristor and chaotic system to handwritten digit recognition [15] and sensor location optimization within a wireless sensor network [16], respectively. Remarkable results were reported [15,16].

As the main component of the biological nervous system, the neuron has been widely studied by many scholars. Some existing neuron models include Hodgkin–Huxley (HH) neuron [17], Hindmarsh–Rose (HR) neuron [18,19], Fitzhugh–Nagumo (FHN) neuron [20], Morris–Lecar (ML) neuron [21], Rulkov model [22], and Hopfield neural network (HNN) model [23–25]. Homogeneous neuron coupling and heterogeneous neuron coupling have received extensive attention from researchers. Li et al. [26] constructed a homogenous coupled network containing two HR neurons and studied the dynamic behavior, Hamiltonian energy, and phase synchronization behavior of the network. The results showed that Hamiltonian energy calculation could not only reveal the firing mechanism of the neural

network but also be used to explore the synchronization control applications of the neural network. Li et al. coupled HR neurons and FHN neurons through memristors to construct a small heterogeneous coupled network, and studied the effects of time delay [27] and external radiation [28] on the heterogeneous coupled network, respectively. The former shows that the two time delays will make the stable equilibrium point unstable, resulting in periodic oscillations known as Hopf bifurcation. Such time delays affect the firing activity of the neural network, and the time delay on different neurons has different effects on synchronization. The latter shows that different initial conditions will generate different bifurcation paths in the network, resulting in various coexisting firing patterns. When the intensity of electromagnetic radiation changes, the network produces opposite bifurcation paths. In addition, it is observed that when the coupling intensity is reduced to a negative value, the two neurons can realize phase synchronization. Njitacke et al. [29] studied the effect of electromagnetic radiation on a heterogeneous coupled network, which has no equilibrium point and, thus, shows hidden dynamic behavior. Ref. [29] also proved that the network has Hamiltonian energy to maintain the electrical activity of neurons. In [30], HR and FHN neurons are coupled into a heterogeneous coupled network through a multistable memristor, which has no equilibrium point and also shows extreme multistability.

Most of the existing studies on heterogeneous coupling focus on HR neurons and FHN neurons. There is a lack of studies on the heterogeneous coupling between HNN and other neurons. Wang et al. [31] realized the heterogeneous coupling of 3D HNN and 2D HR neurons through a memristor and studied the firing behavior and multistability phenomenon of this novel heterogeneous coupled network. In this study, the 2D HNN and 2D HR neurons are coupled through a locally active memristor, and the firing behavior, coexistence phenomenon, and phase synchronization of the network are studied. More specifically, we use a 2D HNN to simulate a specific functional brain region in the brain, HR neurons to simulate their connected neurons, and a memristor to simulate the synapses between two neurons. Based on this, we build a small heterogeneous coupled network that exhibits multiple firing modes, multiple periodic bursters with different spikes, and coexistence. Interestingly, we also find that the phase synchronization behavior of the network is different from other networks, that is, when the coupling intensity gradually increases, the network changes from synchronization to asynchronous and suddenly changes to synchronization when the coupling intensity k_1 is near the value of 1.96. We believe that this abnormal phase synchronization behavior is related to epilepsy and other diseases. This helps us further understand the mechanism of biological brain activity. However, because the number of HNN neurons examined in this study is too small, while the number of neurons in the brain is large, the behavior of a small network is sometimes different from that of a large network, so some statements in this paper are conjecture and need to be further verified by experiments. This work also lays a foundation for the next stage of our research on fraction-order heterogeneous coupled networks, where we will compare the similarities and differences between integer-order heterogeneous coupled networks and fraction-order heterogeneous coupled networks, and explore the potential uses of both. In addition, we also design the simulation circuit of the network to verify the physical realizability of the system.

The rest of this paper is organized as follows: In Section 2, a novel small heterogeneous coupled network is proposed. Section 3 reveals the firing modes and phase synchronization of the network. In Section 4, the network is simulated in a Multisim environment and, subsequently, implemented on an STM32 microcomputer. Section 5 summarizes this article.

2. Mathematical Model and Equilibrium Point Studies

2.1. Mathematical Model

Neurons in the human brain are numerous and complex. Information needs to be transmitted between different brain regions or between brain regions and external neurons. This process often involves different types of neurons. Thus, the study of a heterogeneous coupled network is essential. We use a locally active memristor as a memristive synapse

to couple 2D HNN and 2D HR neurons to construct a heterogeneous coupled network. Equation (1) is the memristor’s mathematical model.

$$\begin{cases} i = k_1(\tanh(x) + c_0)v \\ \frac{dx}{dt} = v \end{cases} \tag{1}$$

To facilitate the study of the properties of the memristor, we assume $c_0 = 0.01$ and $k_1 = 1$ (c_0 is a constant and k_1 is a variable.) In Equation (1), v , i , and t are considered the input voltage, output current, and time constant, respectively. The pinched hysteresis loops of the memristor model are shown in Figure 1, where A , F , and $x(0)$ stand for the amplitude, frequency, and initial value, respectively. Keeping $A = 1.9$, $F = 0.5$, and the initial state of the memristor unchanged. The results show that the memristor is locally active.

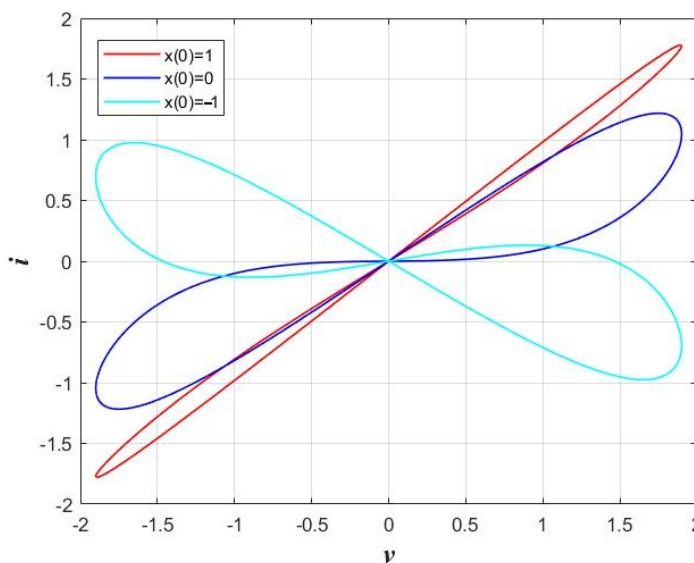


Figure 1. Pinched hysteresis loops with $A = 1.9$, $F = 0.5$, and different initial values.

The mathematical expression of a 2D HR neuron is given as follows:

$$\begin{cases} \frac{dx}{dt} = y - ax^3 + bx^2 + I \\ \frac{dy}{dt} = c - dx^2 - y \end{cases} \tag{2}$$

In Equation (2), x , y , and I denote the membrane potential, relevant recovery variable, and external stimulation current, respectively, where $a = 1$, $b = 3$, $c = 1$, and $d = 5$. The generic HNN model is expressed as follows:

$$C_i \dot{x}_i = -\frac{x_i}{R_i} + \sum_{j=1}^n w_{ij} \tanh(x_j) + I_i \quad (i, j \in N^*) \tag{3}$$

where the resistance, voltage, and capacitance on the membrane of the neuron are denoted using R_i , x_i , and C_i , respectively. In Equation (3), $n = 2$, $\tanh(\cdot)$, w_{ij} , and I_i stand for the neuron activation function, synaptic weight (represents how closely two neurons are connected to each other), and current entering the network, respectively. In Equation (4), we obtain the novel small heterogeneous coupled network’s mathematical expression by setting $C_i = 1$, $R_i = 1$, and $I_i = 0$ in Equation (3).

$$\begin{cases} \frac{dx}{dt} = y - x^3 + 3x^2 + I + k_1(\tanh(n) + 0.01)(x - z) \\ \frac{dy}{dt} = 1 - 5x^2 - y \\ \frac{dz}{dt} = -z - 3.5\tanh(z) + 0.1\tanh(u) - k_1(\tanh(n) + 0.01)(x - z) \\ \frac{du}{dt} = -u - 0.1\tanh(z) + 0.6\tanh(u) \\ \frac{dn}{dt} = x - z \end{cases} \quad (4)$$

In order to facilitate readers to more intuitively understand the network listed in Equation (4), we draw a schematic diagram of its general structure in Figure 2. In Equation (4), the closeness between the HR neuron and HNN is denoted using k_1 . The voltage and recovery variable on the membrane of the HR neuron is denoted using x and y , respectively. I is the external stimulation current, and the voltages on the cell membrane of the neuron 1 and 2 in Figure 2 are denoted using z and u , respectively. The magnetic flux within the network is denoted using u . We set $I = 0$.

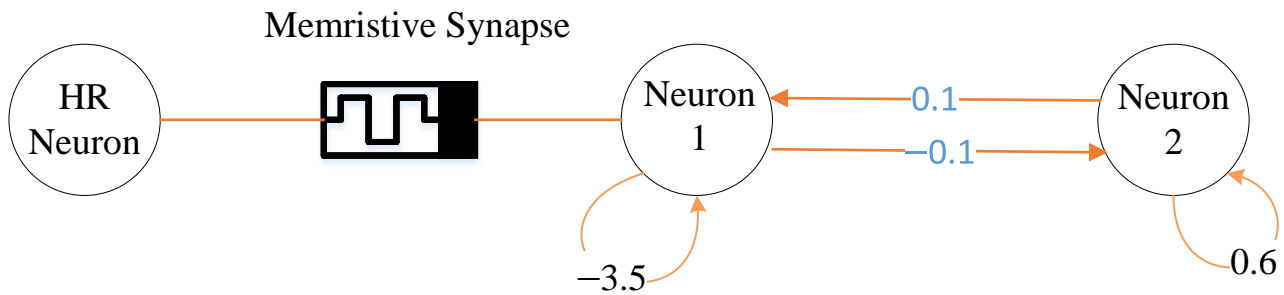


Figure 2. Topology diagram of the novel small heterogeneous coupled network.

2.2. The Equilibrium Points of the Small Heterogeneous Coupled Network

The calculation results of the equilibrium point will reveal the dynamic characteristics of the network. In the same way that self-excited dynamics correspond without a stable equilibrium point, the absence of the equilibrium point often means that a system exhibits hidden dynamics. In order to calculate the network’s equilibrium point, we let $\dot{x} = \dot{y} = \dot{z} = \dot{u} = \dot{n} = 0$; then, Equation (5) is obtained:

$$\begin{cases} y - x^3 + 3x^2 + k_1(\tanh(n) + 0.01)(x - z) = 0 \\ 1 - 5x^2 - y = 0 \\ -z - 3.5\tanh(z) + 0.1\tanh(u) - k_1(\tanh(n) + 0.01)(x - z) = 0 \\ -u - 0.1\tanh(z) + 0.6\tanh(u) = 0 \\ x - z = 0 \end{cases} \quad (5)$$

The Jacobian matrix is shown in Equation (6).

$$J = \begin{pmatrix} W_1 & 1 & -k_1(\tanh(n) + 0.01) & 0 & W_3 \\ -10x & -1 & 0 & 0 & 0 \\ -k_1(\tanh(n) + 0.01) & 0 & W_2 & 0.1(1 - \tanh^2(u)) & -W_3 \\ 0 & 0 & -0.1(1 - \tanh^2(z)) & -1 + 0.6(1 - \tanh^2(u)) & 0 \\ 1 & 0 & -1 & 0 & 0 \end{pmatrix} \quad (6)$$

$$\begin{cases} W_1 = 6x - 3x^2 + k_1(\tanh(n) + 0.01) \\ W_2 = -1 - 3.5(1 - \tanh^2(z)) + k_1(\tanh(n) + 0.01) \\ W_3 = k_1(x - z)(1 - \tanh^2(n)) \end{cases} \quad (7)$$

The result of solving Equation (5) illustrates that we cannot find the real solution of the network. Therefore, the network will present hidden dynamic behavior because it is without an equilibrium point.

3. Numerical Simulation

3.1. Firing Activity of the Small Heterogeneous Coupled Network

For revealing the fundamental properties of the network, some classic nonlinear analytical means are indispensable. The use of graphs helps to visually show the impact of certain parameters on the network. We introduce a bifurcation diagram to illustrate the dynamic behavior of an HR neuron inside the network, where x stands for the membrane potential on the neuron in Figure 3a. Apparently, the system is period, and then enters into chaos through forward period-doubling bifurcation, then exits from chaos through reverse period-doubling bifurcation and enters into period behavior. In Figure 3b, the maximum Lyapunov exponent is a positive number when $0.69 < k_1 < 1.55$, which is powerful evidence that the network is in chaos. In Figure 4, the number of spikes in bursting firing can be controlled by changing the value of k_1 , that is, the coupling strength of synapses affects the number of spikes in bursting firing. Obviously, the coupling strength of synapses between neurons affects the excitability of the nervous system, which provides a way to understand how the excitability of the nervous system affects the duration of emotions. In Figure 5, the increase in synaptic connection strength k_1 causes the network to generate five firing modes, i.e., periodic spiking, chaotic spiking, stochastic bursting, chaotic bursting, and periodic bursting. A disparate attractor shape implies a disparate firing mode, and five disparate attractors are displayed in Figure 6. Figure 7a shows the coexisting attractor phase diagram of the network with disparate initial values. The green curve in the figure illustrates that the network is in chaos, and it is in the period state when the blue curve appears. Figure 7b shows the basin of attraction for the coexisting behavior. The dark blue represents that the system is in a periodic state, and the light blue represents that the system is in a chaotic state.

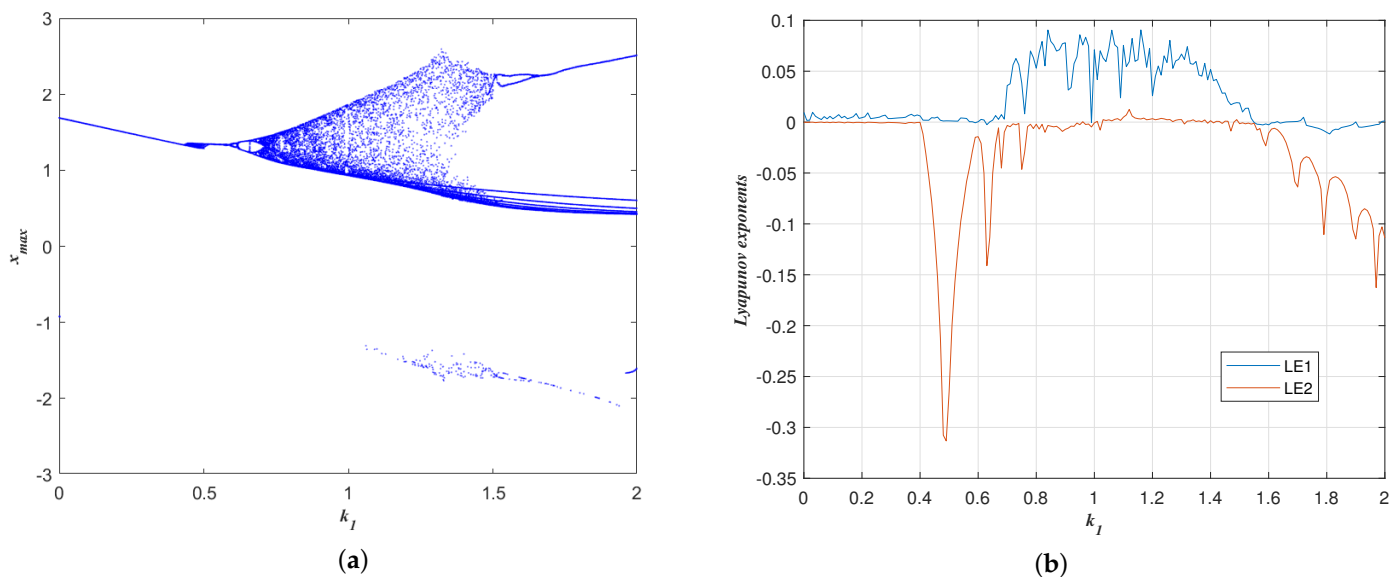


Figure 3. Bifurcation diagram and the two largest Lyapunov exponents of the coupled network controlled by k_1 , with initial states $(0.1, 0, 0, 0, 0.1)$. (a) Bifurcation diagram; (b) Lyapunov exponents diagram.

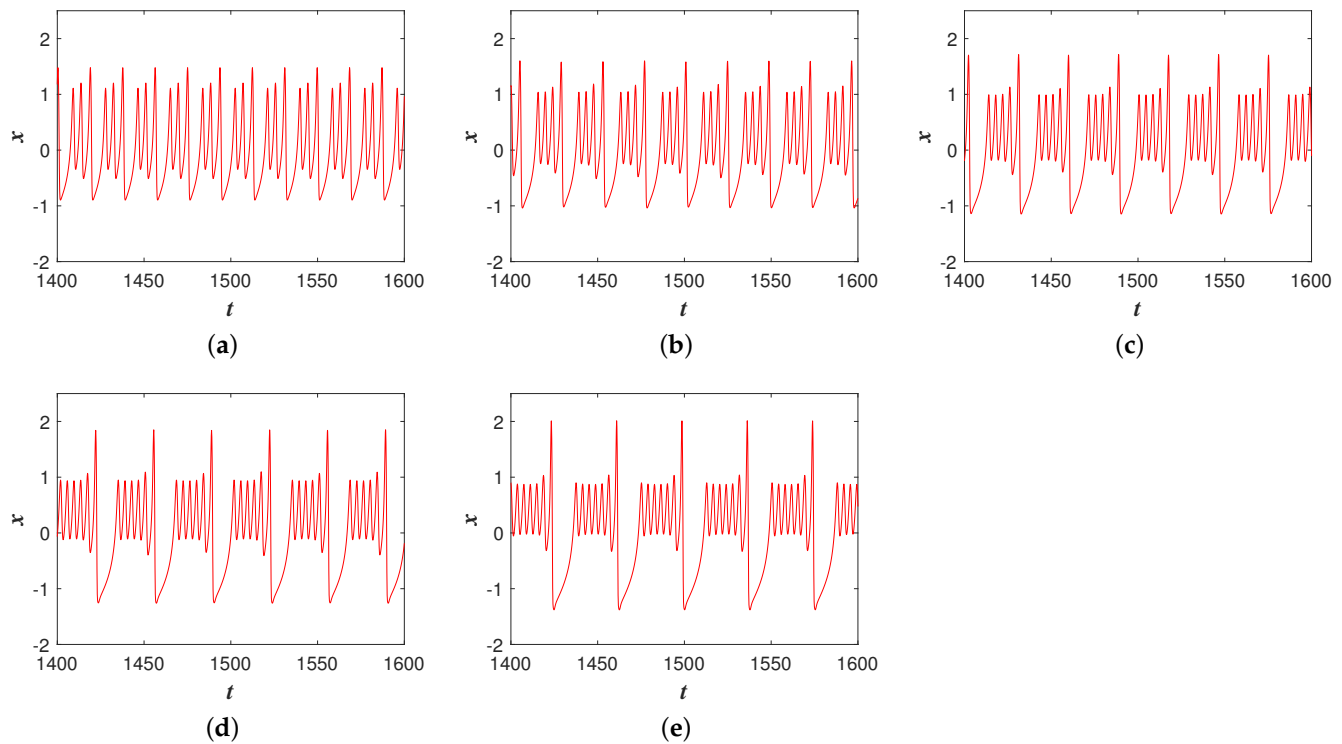


Figure 4. Multiple periodic burstings with different spikes of a small heterogeneous coupled network controlled by k_1 , and initial states $(0.1, 0, 0, 0, 0.1)$. (a) period-3 bursting with $k_1 = 0.75$; (b) period-4 bursting with $k_1 = 0.84$; (c) period-5 bursting with $k_1 = 0.91$; (d) Period-6 bursting with $k_1 = 0.99$; (e) period-7 bursting with $k_1 = 1.083$.

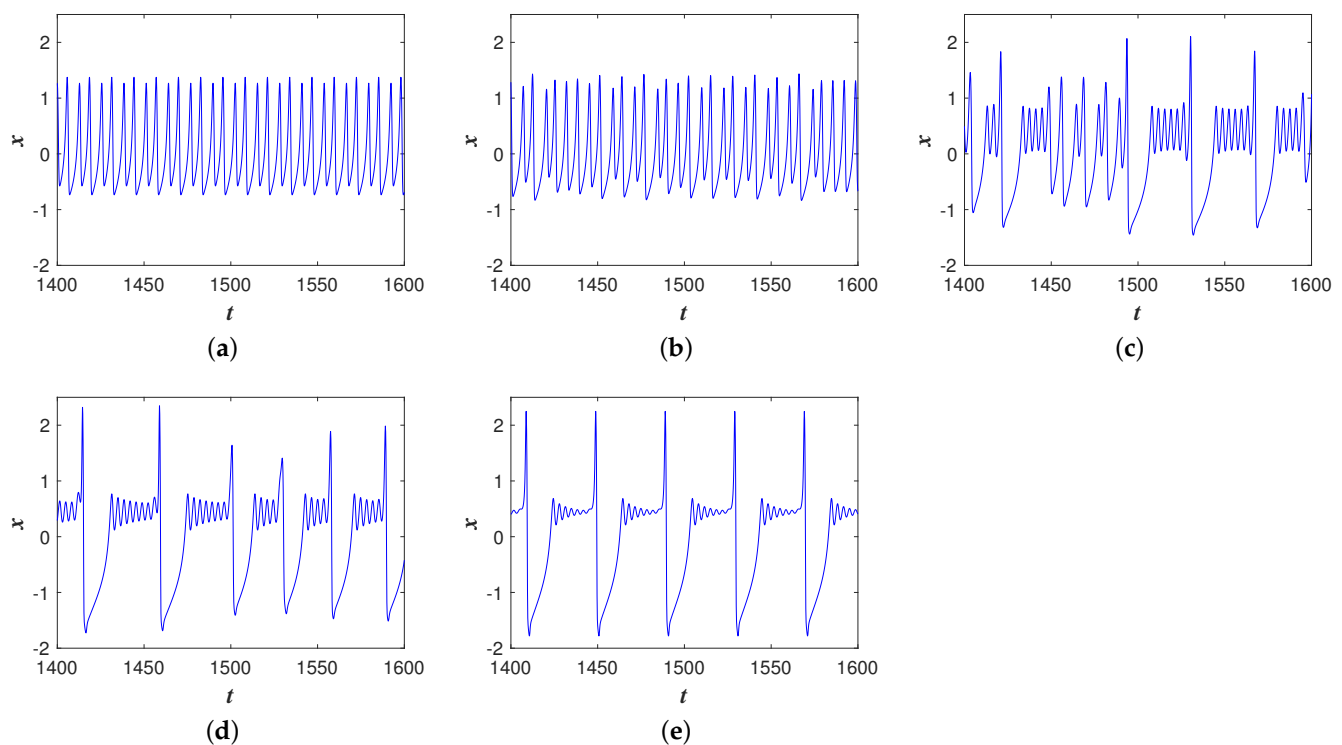


Figure 5. The firing patterns of the membrane potential in a small heterogeneous coupled network controlled by k_1 , with initial states $(0.1, 0, 0, 0, 0.1)$. (a) Periodic spiking mode with $k_1 = 0.63$; (b) chaotic spiking mode with $k_1 = 0.71$; (c) stochastic bursting mode with $k_1 = 1.178$; (d) chaotic bursting mode with $k_1 = 1.39$; (e) periodic bursting mode with $k_1 = 1.65$.

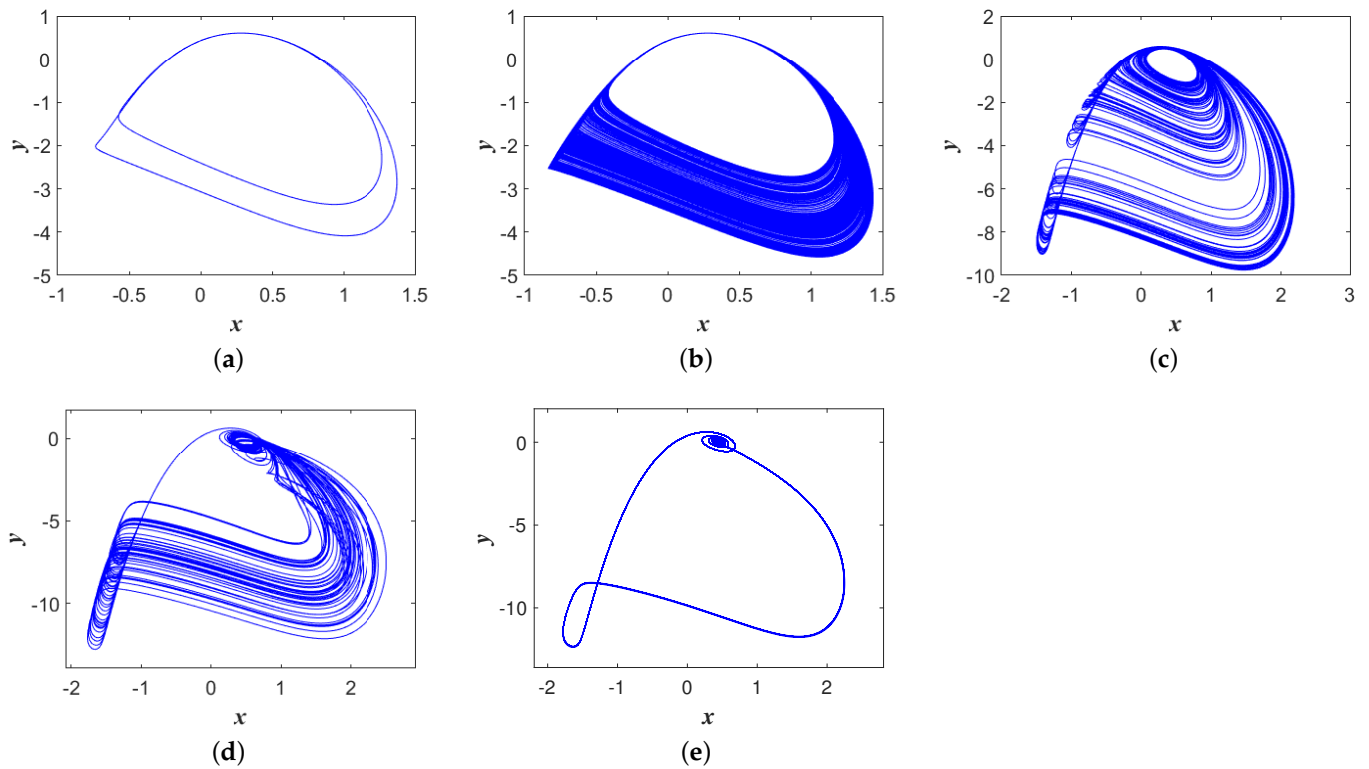


Figure 6. The phase diagrams of the coupled network controlled by k_1 , with initial states (0.1, 0, 0, 0, 0.1). (a) Periodic spiking mode with $k_1 = 0.63$; (b) chaotic spiking mode with $k_1 = 0.71$; (c) stochastic bursting mode with $k_1 = 1.178$; (d) chaotic bursting mode with $k_1 = 1.39$; (e) periodic bursting mode with $k_1 = 1.65$.

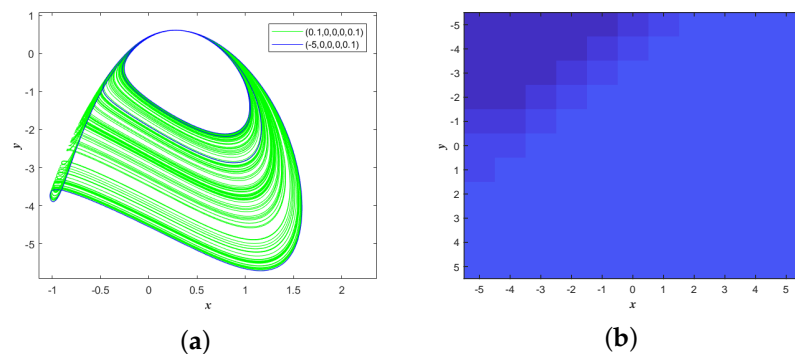


Figure 7. Coexistence behavior controlled by initial value, and $k_1 = 0.83$. (a) The coexisting attractor phase diagram of the network; (b) the basin of attraction for the coexisting behavior.

3.2. Synchronization Behavior of the Small Heterogeneous Coupled Network

Abnormal synchronized behavior in the brain is thought to have certain adverse effects on the nervous system, possibly leading to illnesses such as epilepsy. In this study, we examine the phase synchronization of the heterogeneous neuron coupled system and find that the system shows abnormal synchronization behavior in a certain interval. We have conducted a preliminary study on this abnormal behavior and tried to eliminate this abnormal synchronous behavior by introducing external stimuli. Let us introduce the definition of the burst phase:

$$\theta(t) = 2\pi n + 2\pi \frac{t - t_n}{t_{n+1} - t_n} \quad (t_n < t < t_{n+1}) \tag{8}$$

where t_n is the time when the n -th burst emerges, and $t_{n+1} - t_n$ denotes the burst interval. According to the above definition, every burst leads to a phase increase of 2π . Hence,

phase synchronization can be detected when the absolute value of the phase difference $|\Delta\theta(t)| = |\theta_1(t) - \theta_2(t)|$ between two neurons is bounded with the value of 2π .

We selected some k_1 values to simulate the phase synchronization of the system at these coupling intensities. As shown in Figure 8, when the coupling strength is very small, the system tends to be synchronous, and when the coupling strength increases, the system changes to be asynchronous. Different from the results of previous studies, the system suddenly changes into the synchronous state when $k_1 = 1.96$. Inspired by the fact that the episodic synchronous abnormal firing of excitatory neurons in the hippocampus of the brain can lead to diseases such as epilepsy, it is reasonable to think that this abnormal synchronous behavior can have some adverse effects on the nervous system. We think that adding radiation to the neurons may be able to weaken the possible adverse effects of this abnormal synchronization, but this needs to be confirmed by further experiments.

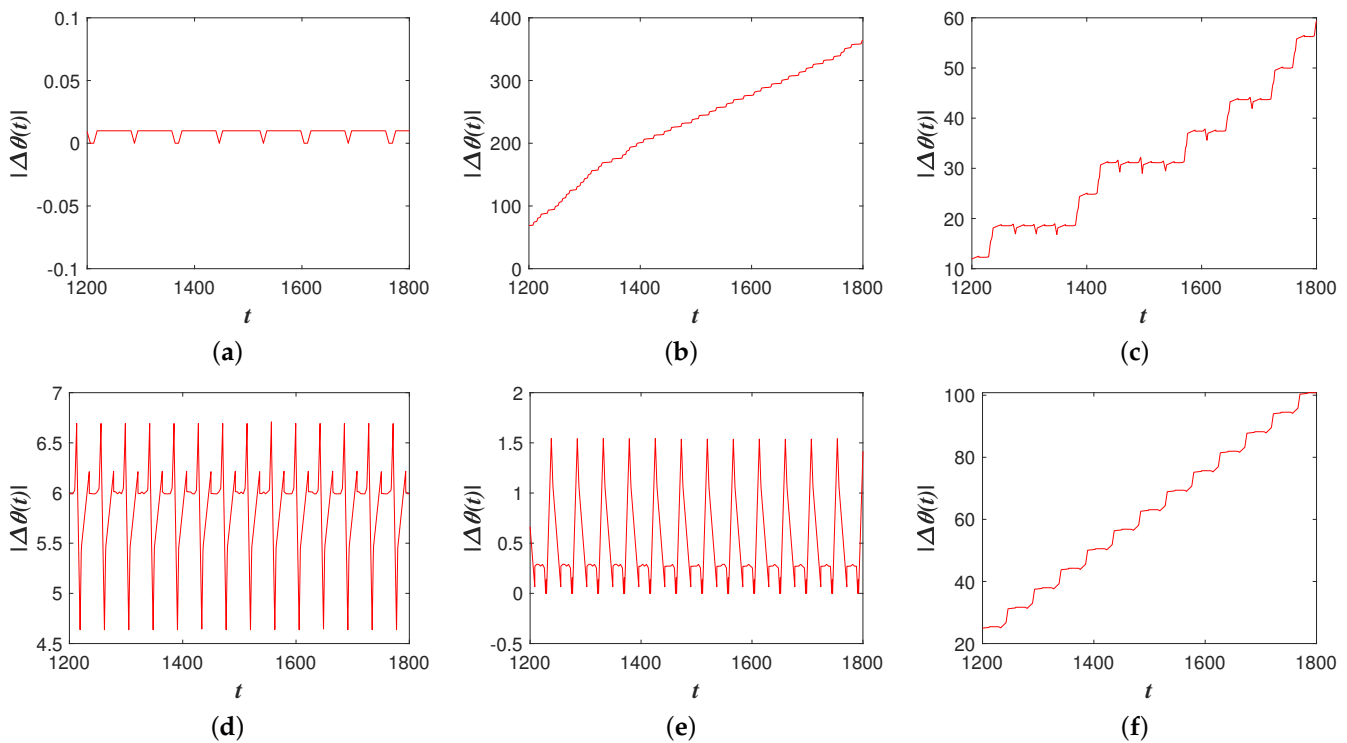


Figure 8. The phase synchronization in a small heterogeneous coupled network controlled by k_1 , with initial states $(0.1, 0, 0, 0, 0.1)$. (a) $k_1 = 0.5$; (b) $k_1 = 0.8$; (c) $k_1 = 1.5$; (d) $k_1 = 1.8$; (e) $k_1 = 1.96$; (f) $k_1 = 1.98$.

4. Circuit Simulation and Hardware Implementation

The physical realization of the network would facilitate its application to industrial production. Therefore, we choose to design the analog circuit of the network on Multisim and verify whether the results of the circuit are consistent with the MATLAB 2021a simulation results. The network will be further implemented on the STM32 microcontroller if they are consistent.

4.1. Circuit Simulation

Through the equivalent substitution of Equation (4), we obtain the circuit expression of the network:

$$\begin{cases} C \frac{dv_x}{dt} = \frac{v_y}{R_1} - \frac{g^2 v_x^3}{R_2} + \frac{g v_x^2}{R_3} + \frac{g k_1 (\tanh(v_n) + 0.01e)(v_x - v_z)}{R_L} \\ C \frac{dv_y}{dt} = \frac{e}{R_5} - \frac{g v_x^2}{R_4} - \frac{v_y}{R_5} \\ C \frac{dv_z}{dt} = -\frac{v_z}{R} + \frac{\tanh(v_z)}{R_6} + \frac{\tanh(v_u)}{R_7} - \frac{g k_1 (\tanh(v_n) + 0.01e)(v_x - v_z)}{R_L} \\ C \frac{dv_u}{dt} = -\frac{v_u}{R} + \frac{\tanh(v_z)}{R_9} + \frac{\tanh(v_u)}{R_{10}} \\ C \frac{dv_n}{dt} = \frac{v_x - v_z}{R_k} \end{cases} \quad (9)$$

Equation (10) illustrates the circuit elements values of the network:

$$\begin{cases} VCC = 5\text{ V}, VEE = -5\text{ V}, R_C = 1\text{ K}\Omega, R_F = 520\ \Omega, I_0 = 1.1\text{ mA} \\ RC = 100\ \mu\text{s}, R_0 = 10\text{ K}\Omega, C = 10\text{ nF}, g = 1, g_{k_1} = k_1 \\ R_1 = 10\text{ K}\Omega, R_2 = 10\text{ K}\Omega, R_3 = 3.33\text{ K}\Omega, R_L = 10\text{ K}\Omega, R_k = 10\text{ K}\Omega \\ R_5 = 10\text{ K}\Omega, R_4 = 2\text{ K}\Omega, R_5 = 10\text{ K}\Omega, E_1 = 1\text{ V}, E_2 = 0.01\text{ V} \\ R_6 = 2.857\text{ K}\Omega, R_7 = 100\text{ K}\Omega, R_8 = 100\text{ K}\Omega, R_9 = 16.667\text{ K}\Omega \end{cases} \quad (10)$$

The simulation circuit of the network is shown in Figures 9 and 10. Figure 9 is the circuit diagram of the hyperbolic tangent function, and the values of the components in Figures 9 and 10 are shown in Equation (10). The amplifiers used in Figures 9 and 10 are TL082CP, and the supply voltages are +15 V and -15 V. The circuit's frequency up to 3 MHz. The multiplier used is the analog multiplier, g represents the multiplier of the two inputs of the factor, and the transistor is 2N2222. The $-\tanh$ module in Figure 10 is the circuit in Figure 9. The simulation results of the Multisim circuit are shown in Figure 11. Obviously, they are consistent with the simulation results of MATLAB 2021a. It is reasonable to think that the circuit in Figure 10 can physically realize the heterogeneous coupled network of Equation (4).

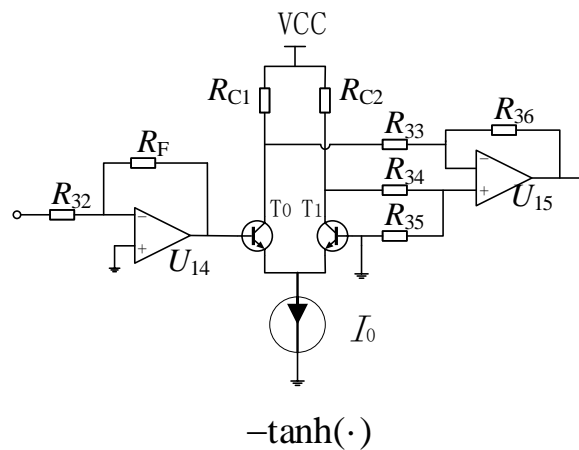


Figure 9. A circuit diagram of the hyperbolic tangent function.

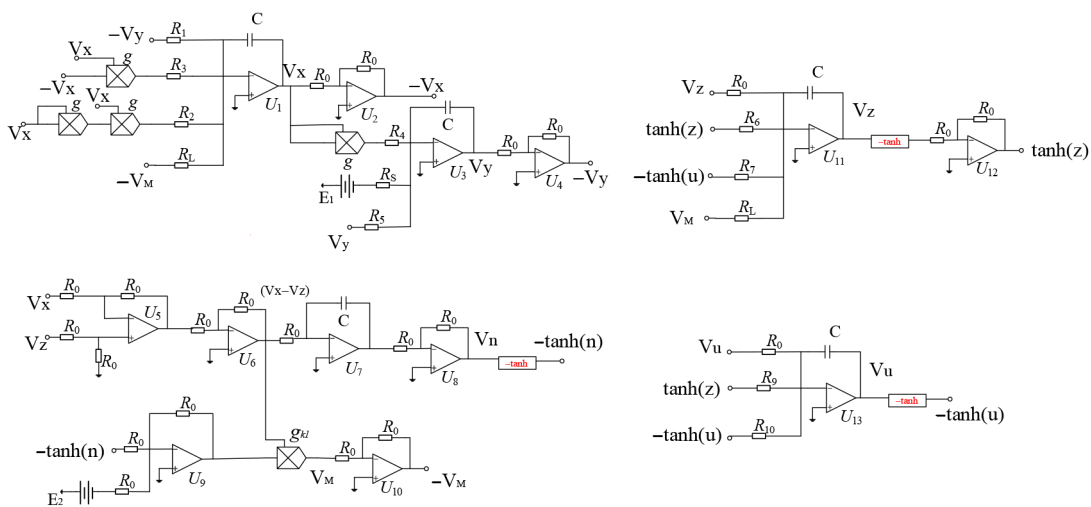


Figure 10. A circuit diagram of the coupled network.

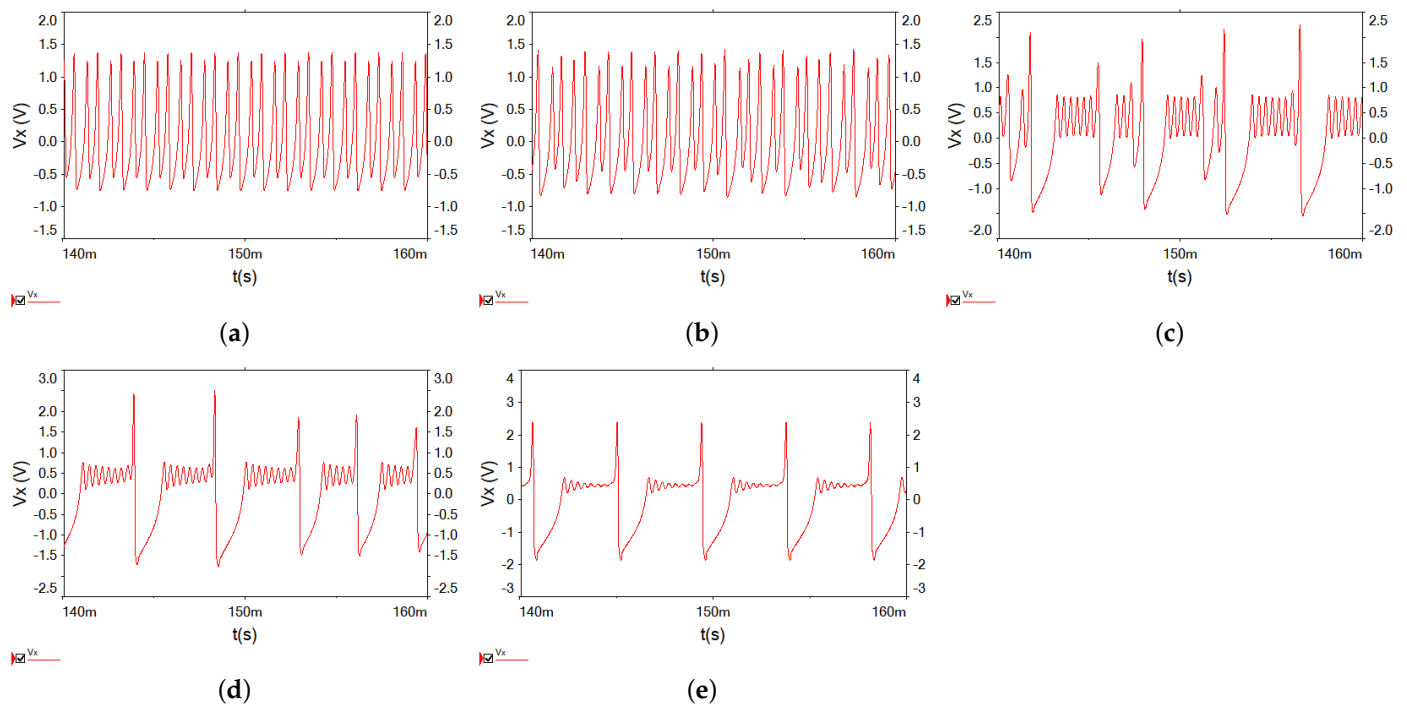


Figure 11. Simulation results of the small heterogeneous coupled network. (a). $k_1 = 0.63$; (b). $k_1 = 0.71$; (c). $k_1 = 1.178$; (d). $k_1 = 1.39$; (e). $k_1 = 1.65$.

4.2. Microcontroller Implementation

A microcontroller is widely used in industry because of its advantages of high speed, compactness, and low cost. In this section, we will use the STM32F407ZGT6 microcontroller to implement this small heterogeneous coupled network and use C language to write programs. It is produced by STMicroelectronics which was formed by the merger of SGS Microelectronics of Italy and Thomson Semiconductor of France, and its headquarters are in Switzerland. It has a frequency up to 168 MHz. The signal generated via the STM32 microcontroller will be displayed on the oscilloscope, and the hardware layout diagram is shown in Figure 12. This small heterogeneous coupled network is mainly implemented using the fourth-order Runge–Kutta algorithm, the approximate flowchart of which is shown in Figure 13. The experimental setup of the small heterogeneous coupled network on the STM32 single-chip microcomputer is shown in Figure 14, and the result is consistent with that in Figure 5. It is reasonable to think that the network is implemented on the single-chip microcomputer.

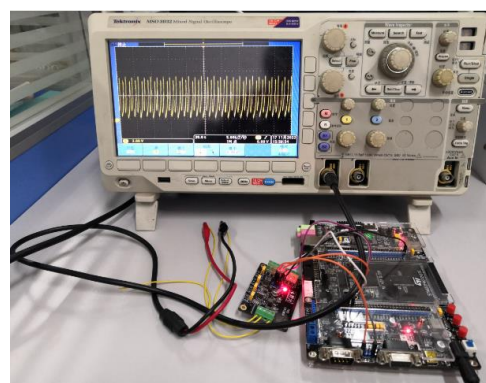


Figure 12. STM32-based hardware layout diagram of the small heterogeneous coupled network.

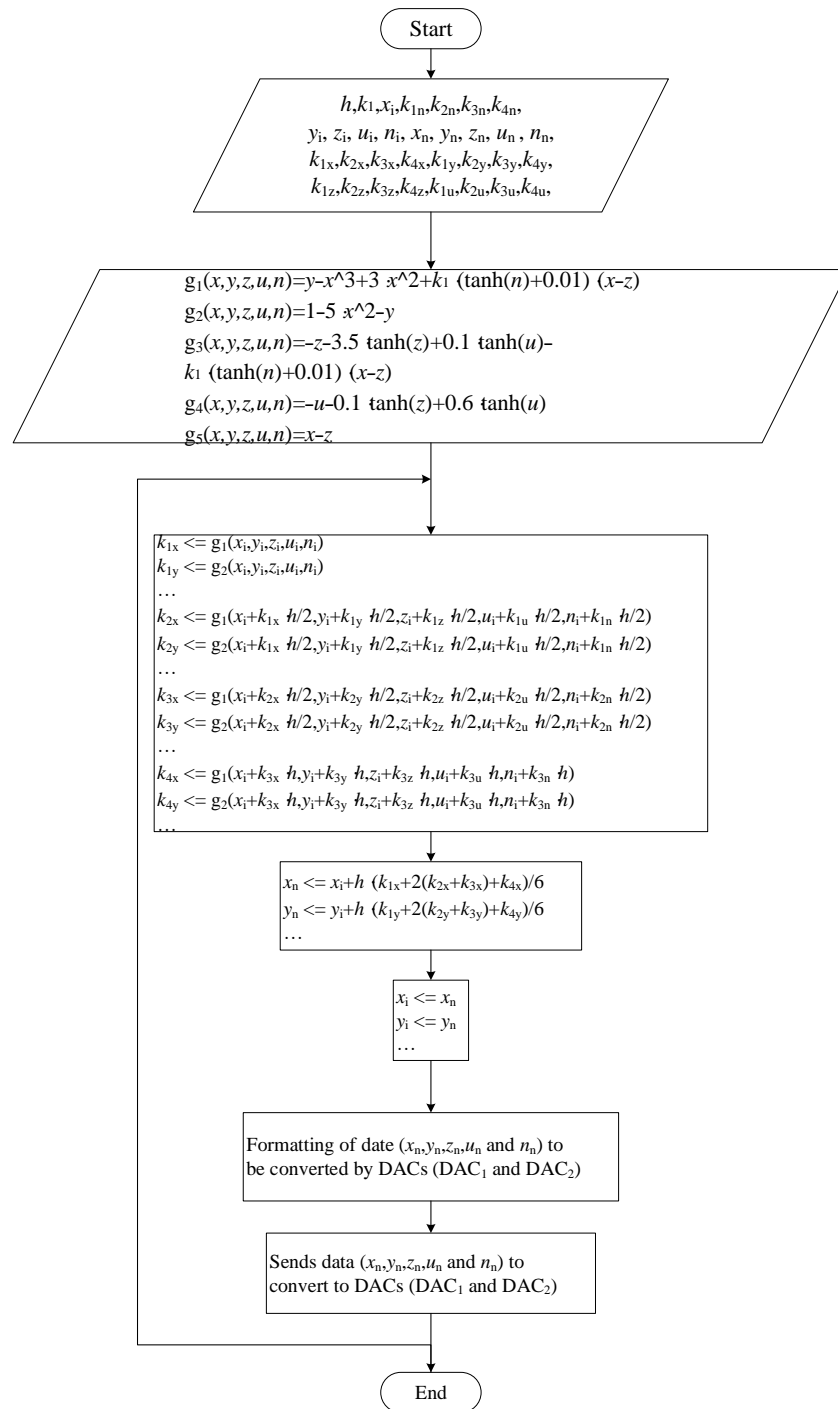


Figure 13. STM32-based flowchart of the fourth-order Runge–Kutta integration method.

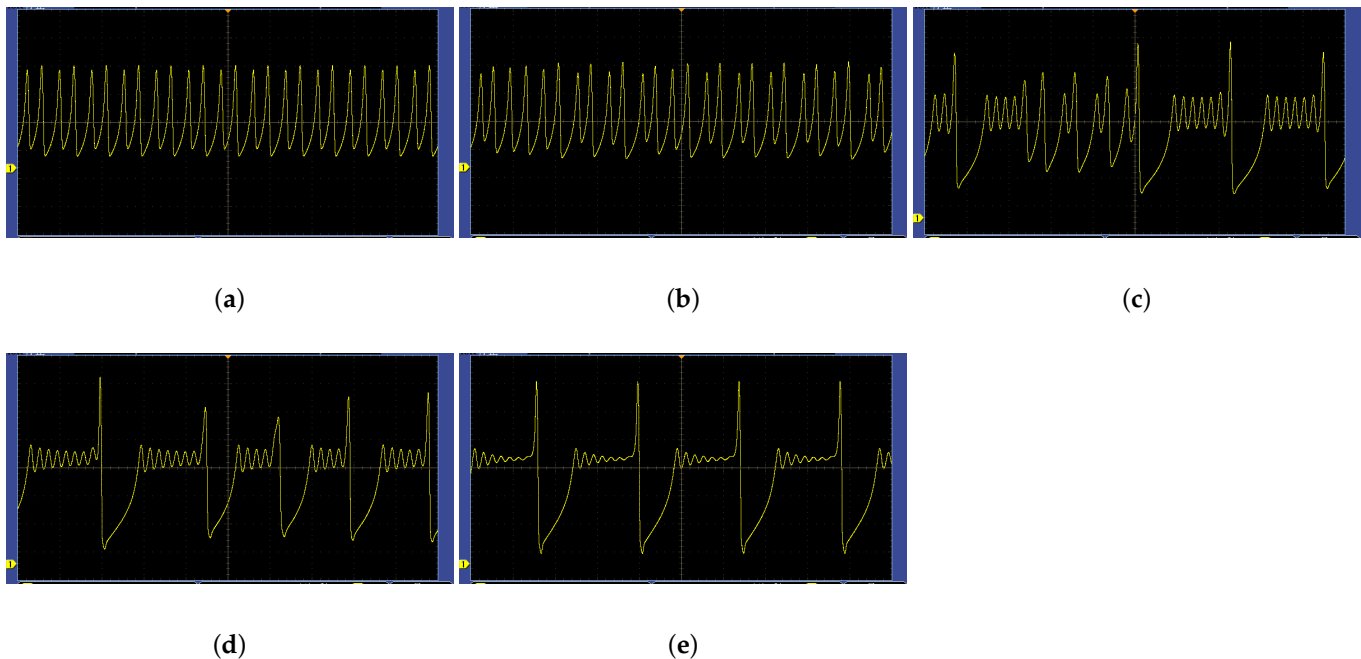


Figure 14. Microcontroller implementation of the small heterogeneous coupled network. (a). $k_1 = 0.63$; (b). $k_1 = 0.71$; (c). $k_1 = 1.178$; (d). $k_1 = 1.39$; (e). $k_1 = 1.65$.

5. Conclusions

This study proposes a novel small heterogeneous coupled network, using a locally active memristor as a memristive synapse to couple 2D HNN and 2D HR neurons. The calculation results show that the network has no equilibrium point and shows hidden dynamics. The novel small heterogeneous coupled network exhibits five stable firing modes as k_1 changes. In addition, in the local region of k_1 , the number of spikes in bursting firing increases with the increase in k_1 . The above phenomenon shows that the firing mode is controlled by the coupling strength and is consistent with the behavior of neurons. More interestingly, when the coupling intensity k_1 increases, the network changes from synchronous to asynchronous, but suddenly changes to synchronous around the coupling parameter $k_1 = 1.96$. This abnormal synchronization behavior is different from previous studies, which provides a new way for us to further understand the mechanism of brain activity. Finally, the network is simulated in Multisim environment and implemented experimentally on STM32.

Author Contributions: Conceptualization, X.Z.; Methodology, M.W. and X.Z.; Software, J.P. and X.Z.; Formal analysis, S.H. and H.H.-C.I.; Investigation, J.P. and H.H.-C.I.; Resources, S.H.; Data curation, X.Z.; Writing—original draft, J.P.; Writing—review & editing, M.W., S.H. and H.H.-C.I.; Supervision, M.W. and S.H.; Project administration, S.H.; Funding acquisition, M.W. All authors have read and agreed to the published version of the manuscript.

Funding: This research was funded by the National Natural Science Foundation of China (Grant No. 62071411 and No. 62171401) and the Research Foundation of Education Department of Hunan Province (Grant No. 20B567).

Data Availability Statement: The datasets generated during and/or analyzed during the current study are available from the corresponding author upon reasonable request.

Conflicts of Interest: The authors declare that they have no conflict of interest.

Abbreviations

The following abbreviations are used in this manuscript:

HR	Hindmarsh–Rose
HNN	Hopfield neural network
2D	Two dimensional

References

- Wang, M.; Deng, Y.; Liao, X.; Li, Z.; Ma, M.; Zeng, Y. Dynamics and circuit implementation of a four-wing memristive chaotic system with attractor rotation. *Int. J. Non-Linear. Mech.* **2019**, *111*, 149–159. [[CrossRef](#)]
- Peng, Y.; He, S.; Sun, K. Parameter identification for discrete memristive chaotic map using adaptive differential evolution algorithm. *Nonlinear Dyn.* **2022**, *107*, 1263–1275. [[CrossRef](#)]
- Li, H.; Li, C.; He, S. Locally Active Memristor with Variable Parameters and Its Oscillation Circuit. *Int. J. Bifurcat. Chaos* **2023**, *33*, 2350032. [[CrossRef](#)]
- Wang, M.; An, M.; Zhang, X.; Iu, H.H.C. Feedback Control-Based Parallel Memristor-Coupled Sine Map and Its Hardware Implementation. *IEEE Trans. Circuits Syst. II-Express Briefs* **2023**, *70*, 4251–4255. [[CrossRef](#)]
- Wang, M.; An, M.; He, S.; Zhang, X.; Ho-Ching Iu, H.; Li, Z. Two-dimensional memristive hyperchaotic maps with different coupling frames and its hardware implementation. *Chaos Interdiscip. J. Nonlinear Sci.* **2023**, *33*, 073129. [[CrossRef](#)] [[PubMed](#)]
- Xu, F.; Zhang, J.; Fang, T.; Huang, S.; Wang, M. Synchronous dynamics in neural system coupled with memristive synapse. *Nonlinear Dyn.* **2018**, *92*, 1395–1402. [[CrossRef](#)]
- Chen, C.; Bao, H.; Chen, M.; Xu, Q.; Bao, B. Non-ideal memristor synapse-coupled bi-neuron Hopfield neural network: Numerical simulations and breadboard experiments. *AEU-Int. J. Electron. Commun.* **2019**, *111*, 152894. [[CrossRef](#)]
- Chen, C.; Chen, J.; Bao, H.; Chen, M.; Bao, B. Coexisting multi-stable patterns in memristor synapse-coupled Hopfield neural network with two neurons. *Nonlinear Dyn.* **2019**, *95*, 3385–3399. [[CrossRef](#)]
- Lin, H.; Wang, C.; Hong, Q.; Sun, Y. A multi-stable memristor and its application in a neural network. *IEEE Trans. Circuits Syst. II-Express Briefs* **2020**, *67*, 3472–3476. [[CrossRef](#)]
- Lin, H.; Wang, C.; Sun, Y.; Yao, W. Firing multistability in a locally active memristive neuron model. *Nonlinear Dyn.* **2020**, *100*, 3667–3683. [[CrossRef](#)]
- Pham, V.T.; Volos, C.; Jafari, S.; Kapitaniak, T. Coexistence of hidden chaotic attractors in a novel no-equilibrium system. *Nonlinear Dyn.* **2017**, *87*, 2001–2010. [[CrossRef](#)]
- Cang, S.; Li, Y.; Zhang, R.; Wang, Z. Hidden and self-excited coexisting attractors in a Lorenz-like system with two equilibrium points. *Nonlinear Dyn.* **2019**, *95*, 381–390. [[CrossRef](#)]
- Pisarchik, A.N.; Feudel, U. Control of multistability. *Phys. Rep.* **2014**, *540*, 167–218. [[CrossRef](#)]
- Parastesh, F.; Jafari, S.; Azarnoush, H. Traveling patterns in a network of memristor-based oscillators with extreme multistability. *Eur. Phys. J. Spec. Top.* **2019**, *228*, 2123–2131. [[CrossRef](#)]
- He, S.; Liu, J.; Wang, H.; Sun, K. A discrete memristive neural network and its application for character recognition. *Neurocomputing* **2023**, *523*, 1–8. [[CrossRef](#)]
- He, S.; Fu, L.; Lu, Y.; Wu, X.; Wang, H.; Sun, K. Analog circuit of a simplified Tent map and its application in sensor position optimization. *IEEE Trans. Circuits Syst. II-Express Briefs* **2022**, *70*, 885–888. [[CrossRef](#)]
- Hodgkin, A.L.; Huxley, A.F. A quantitative description of membrane current and its application to conduction and excitation in nerve. *J. Physiol.* **1952**, *117*, 500. [[CrossRef](#)] [[PubMed](#)]
- Hindmarsh, J.L.; Rose, R.M. A model of the nerve impulse using two first-order differential equations. *Nature* **1982**, *296*, 162–164. [[CrossRef](#)]
- Hindmarsh, J.L.; Rose, R.M. A model of neuronal bursting using three coupled first order differential equations. *Proc. R. Soc. Lond. Ser. Biol. Sci.* **1984**, *221*, 87–102.
- Izhikevich, E.M.; FitzHugh, R. Fitzhugh-nagumo model. *Scholarpedia* **2006**, *1*, 1349. [[CrossRef](#)]
- Tsumoto, K.; Kitajima, H.; Yoshinaga, T.; Aihara, K.; Kawakami, H. Bifurcations in Morris-Lecar neuron model. *Neurocomputing* **2006**, *69*, 293–316. [[CrossRef](#)]
- Ma, M.; Lu, Y.; Li, Z.; Sun, Y.; Wang, C. Multistability and Phase Synchronization of Rulkov Neurons Coupled with a Locally Active Discrete Memristor. *Fractal Fract.* **2023**, *7*, 82. [[CrossRef](#)]
- Hopfield, J.J. Neural networks and physical systems with emergent collective computational abilities. *Proc. Natl. Acad. Sci. USA* **1982**, *79*, 2554–2558. [[CrossRef](#)] [[PubMed](#)]
- Hopfield, J.J. Neurons with graded response have collective computational properties like those of two-state neurons. *Proc. Natl. Acad. Sci. USA* **1984**, *81*, 3088–3092. [[CrossRef](#)]
- Lin, H.; Wang, C.; Chen, C.; Sun, Y.; Zhou, C.; Xu, C.; Hong, Q. Neural bursting and synchronization emulated by neural networks and circuits. *IEEE Trans. Circuits Syst. I-Regul. Pap.* **2021**, *68*, 3397–3410. [[CrossRef](#)]
- Lu, Y.; Li, H.; Li, C. Electrical activity and synchronization of memristor synapse-coupled HR network based on energy method. *Neurocomputing* **2023**, *544*, 126246. [[CrossRef](#)]

27. Guo, Z.; Li, Z.; Wang, M.; Ma, M.L. Hopf bifurcation and phase synchronization in memristor-coupled Hindmarsh–Rose and FitzHugh–Nagumo neurons with two time delays. *Chin. Phys. B* **2023**, *32*, 038701. [[CrossRef](#)]
28. Peng, C.; Li, Z.; Wang, M.; Ma, M. Dynamics in a memristor-coupled heterogeneous neuron network under electromagnetic radiation. *Nonlinear Dyn.* **2023**. [[CrossRef](#)]
29. Njitacke, Z.T.; Tsafack, N.; Ramakrishnan, B.; Rajagopal, K.; Kengne, J.; Awrejcewicz, J. Complex dynamics from heterogeneous coupling and electromagnetic effect on two neurons: Application in images encryption. *Chaos Solitons Fractals* **2021**, *153*, 111577. [[CrossRef](#)]
30. Njitacke Tabekoueng, Z.; Shankar Muni. S.; Fozin Fozin. T.; Dolvis Leutcho, G.; Awrejcewicz, J. Coexistence of infinitely many patterns and their control in heterogeneous coupled neurons through a multistable memristive synapse. *Chaos Interdiscip. J. Nonlinear Sci.* **2022**, *32*, 053114. [[CrossRef](#)]
31. Wang, M.; Peng, J.; Zhang, X.; Iu, H.H.C.; Li, Z. Firing activities analysis of a novel small heterogeneous coupled network through a memristive synapse. *Nonlinear Dyn.* **2023**, *111*, 15397–15415. [[CrossRef](#)]

Disclaimer/Publisher’s Note: The statements, opinions and data contained in all publications are solely those of the individual author(s) and contributor(s) and not of MDPI and/or the editor(s). MDPI and/or the editor(s) disclaim responsibility for any injury to people or property resulting from any ideas, methods, instructions or products referred to in the content.